

Simulation of Earthquake Ground Motion and Effects on Engineering Structures during the Preruptive Phase of an Active Volcano

by Gaetano Festa, Aldo Zollo, Gaetano Manfredi, Maria Polese, and Edoardo Cosenza

Abstract Several of the world's active volcanoes are located near densely populated areas, and therefore the seismic hazard associated with preruptive earthquake activity and its relation to the potential damage of engineering structures should be considered as a part of risk evaluation and management. This is true for Mt. Vesuvius volcano (southern Italy), where several hundred thousand people are exposed to volcanic and related seismic risks. This study investigates the effect of preruptive seismic activity through the massive simulation of earthquake waveforms in the magnitude, location, and focal-mechanism ranges expected for Mt. Vesuvius seismicity. Synthetics are processed to evaluate the characteristic strong-motion parameters, which are useful for estimating the seismic damage to a built-up environment that would arise from both the maximum expected single event and the cumulative effect of a large number of small events. Synthetic and observed strong-motion parameters for a selected set of recorded earthquakes are compared to validate the modeling approach. The scaling of the simulated peak ground acceleration (PGA) with distance appears to be influenced by earthquake depth, owing to the presence of a sharp velocity discontinuity at shallow depths underneath the Vesuvius area. On the other hand, the hysteretic energy spectrum, related to the plastic behavior of the structures, depends strongly on the b -parameter of the Gutenberg–Richter law (G–R). By varying the G–R law parameters across a reasonable expected range, we observe that the cumulative hysteretic energy is comparable to the values observed at near-source distances during the 1997 Umbria-Marche, Italy, event (M 5.8), which produced serious damage to buildings and infrastructure, although a significant PGA value was not recorded.

Introduction

To estimate the risk from volcanic activity, any potential loss or damage to population, property, and buildings needs to be evaluated. In general, volcanic hazard refers to the probability of the occurrence of a given eruption event, and it is essentially based on the expected eruption scenario. Whereas superficial and evident phenomena that usually accompany an eruption (such as lava and pyroclastic flow, ash, volcanic gases, landslides and tsunamis, and lahars) are commonly considered to be responsible for volcanic hazards, the influence of volcanic earthquakes still has to be clearly understood and accounted for in the framework of a multi-risk approach to the problem of volcanic-risk evaluation and management. This paper is aimed at providing an insight into volcanic hazards from both the seismological and structural-engineering points of view. This is relevant for volcanoes located near densely populated urban areas because it links the hazards to the potential damage of a built-up environment in a multi-risk-evaluation approach.

The topic was dealt with by investigating the potential

damage of preruptive earthquakes that would precede a possible eruption of Mt. Vesuvius volcano. This volcano is in a densely populated area, 20 km west of Naples in southern Italy, where more than a million inhabitants live. At present, this volcano is continuously monitored by the Osservatorio Vesuviano (INGV) by using an advanced multidisciplinary array of geophysical and geochemical instruments that continually analyze the background volcanic activity in the search for any anomalous changes that could announce an impending eruptive event. An emergency plan has been designed and implemented by the local authorities to ensure the immediate and safe evacuation of the population. As a consequence, the full serviceability of the infrastructure would be of great importance during the preruptive phase.

The risk for the Vesuvius area is high because of the large vulnerability and exposure factors, which are increased by the presence of several densely built-up and populated towns in a relatively limited zone. Moreover, the structures

have been almost entirely built following unsatisfactory design criteria and with low-quality materials. Most of the reinforced-concrete structures that were built in the 1960s and 1970s have been designed only for gravity loads; as a consequence, buildings will be particularly vulnerable, and the existing transportation facilities may be put out of service in an emergency.

The potential damage of an earthquake is usually assessed with the aid of selected, representative ground motion and spectral parameters. During the evolution of a volcanic system from a quiescent state to an eruptive state, a large number of small- to moderate-sized earthquakes occur. Thus, the cumulative effects of these numerous, though small-magnitude, earthquakes can also cause structural damage from the low-cycle fatigue phenomena. Therefore, a global response of the system to the cumulative effects of an earthquake sequence should be considered.

To evaluate the hazard of an active seismic area, the magnitude of the maximum expected earthquake is usually determined from the historical catalog and from instrument recordings. This magnitude is used to estimate the ground-motion parameters, such as PGA, peak ground displacement (PGD), and spectral ordinates, along with consideration of the known attenuation laws (Reiter, 1991). This classical approach cannot be used in this study because a record of an entire preeruptive phase for the Vesuvius area is not available, which prevents an empirical assessment of the expected time and magnitude evolution of preeruptive seismicity. Moreover, we were interested in investigating both the effects of a single earthquake and the cumulative effects of a large number of small- to moderate magnitude events. Finally, for Mt. Vesuvius the magnitude range of the recorded earthquakes is outside the interval generally considered by standard attenuation laws (4.6–7) estimated for Italy (Sabetta and Pugliese, 1987). For these reasons, we decided to base our study on a synthetic waveform database simulating the preeruptive seismic activity. This was processed to obtain structural responses in terms of the relevant ground-motion parameters.

Volcanic Earthquakes

In the evolution of volcanic systems from the quiescent state to eruption, a large number of small- to moderate magnitude earthquakes can occur. While tectonic earthquakes are generally related to a shear-faulting mechanism, volcanic earthquakes may involve tensile, isotropic, and/or shear rock fractures, driven by the percolation of high-temperature fluids/gases or directly by the magma-ascent mechanism. Earthquakes caused by volcanic activity are generally classified into four categories: volcano-tectonic (VT) earthquakes, long-period (LP) earthquakes, harmonic tremor (T), and surface events (SEs) (Minakami, 1974; Benoit and McNutt, 1994).

From the point of view of seismic-hazard analysis in the preeruptive phase, only the VT earthquakes need be consid-

ered. Indeed, both SEs and T generally appear during an eruption, and they have very low amplitudes beforehand. Although LP earthquakes could be present in the pre-eruptive phase, high-magnitude events of such a class are rarely observed before an eruption (Chouet *et al.*, 1994). Moreover, LP earthquakes involve only low-frequency signals, and they are not associated with a well-understood source mechanism.

Construction of a Synthetic Database

In the case of Mt. Vesuvius, the last eruption occurred in 1944, and no detailed information is available relating to the time evolution of its seismic activity (number, location, or magnitude of earthquakes) preceding the eruption. Hence, to provide an estimation of the seismic hazards, a synthetic earthquake catalog was built, and the ground motion in the area was simulated from existing knowledge of the volcanic structure, earthquake locations/mechanisms, and frequency/magnitude occurrences at Mt. Vesuvius and at other volcanoes around the world.

Magnitude Catalog

To describe the scaling of the number of events with magnitude, we have used the Gutenberg–Richter law ($\log_{10} N = a - bM$), where N is the number of events for an assigned magnitude value M . The parameters a and b are generally inferred from a magnitude catalog and can differ from one seismogenetic zone to another. In an active volcanic region, we would expect a variation of b and a values with time preceding and following the eruption, reflecting the natural evolution of the volcano from quiescence to eruption. As a consequence, a local in-time Gutenberg–Richter (G–R) relation should be used for the volcanic areas (De Natale *et al.*, 1985).

To build a synthetic catalog, a probabilistic approach was followed by randomly extracting a series of magnitude values from an assumed G–R distribution. Let M_0 be the minimum magnitude value contained in the catalog (any earthquake with a magnitude smaller than M_0 is supposed to have no significant effect on structures). If the G–R relation is interpreted as a probability distribution function,

$$P(M) = A10^{-bM}. \quad (1)$$

The normalization factor A ($A = 10^a$, by similarity with the G–R relationship) is obtained by imposing the condition:

$$\int_{M_0}^{\infty} A10^{-bM} dM = 1. \quad (2)$$

Formally, the catalog is defined by a sequence of N_{M_0} events of magnitude $M > M_0$, obeying the distribution $P(M)$. Since standard random-number generators provide a succession of values in $[0,1]$, having a uniform distribution, we use the

inverse transform method (see, e.g., Bury, 1975) to allow the simulation of random values $M > M_0$, obeying the probability distribution $P(M)$. If u is a random number in $[0,1]$, the mapping is described by the following relationship:

$$M = M_0 - \frac{1}{b} \log_{10} u. \quad (3)$$

Therefore, the synthetic catalog can be built, assigning a numerical value to two parameters: the b -value and the dimension of the catalog N_{M_0} , which can be directly related to the a parameter of the G–R relationship.

In this study, the expected ranges for both N_{M_0} and b were inferred from the present seismicity of Mt. Vesuvius and from observations of other volcanoes during their preeruptive phases. In volcanic areas, b is generally more variable and higher on average in comparison with b -values observed in tectonic areas (Minakami, 1974). During the 1992 Mt. Spurr, Alaska, eruption, b ranged from 0.75 to 1.8, whereas for the 1980 Mt. St. Helens, Washington, eruption, the range of b was $[0.6, 1.36]$ (Wiemer and McNutt, 1997). Larger values of b were observed for the 1995 Soufriere Hills, Monserrat, eruption ($b = 3.07$; Power *et al.*, 1998) and for the 1981 Mt. Etna, Italy, eruption ($b = 2.00$ – 3.28 ; De Natale *et al.*, 1985). These values are compared with the present $b = 1.1$, obtained at Mt. Vesuvius (Zollo *et al.*, 2002).

The estimation of the b -value during a preeruptive phase at Mt. Vesuvius is arbitrary, since no data are available from historical events. Nevertheless, an increase in b approaching the eruption is expected as a consequence of the magma rising and percolating, which should favor the creation of small-scale seismic fractures. For this study, we set $b = 2$.

We used $M_0 = 2$ as the minimum magnitude value for the catalog. This choice was validated *a posteriori*, observing that PGA values decrease proportionally to the seismic moment (Fig. 1) and plastic effects produced by very low energy events can be considered negligible.

Finally, the number of events N_{M_0} , with magnitude $M > M_0$, was chosen in accord with observations of other volcanoes because no data from Mt. Vesuvius are available for this purpose (the last eruption occurred in 1944). Complete catalogs for significant eruptions are available for Mt. St. Helens (eruption of 1980) and Mt. Redoubt (eruption of 1989). In the first case, about 600 earthquakes of magnitudes >3 were recorded before the Plinian, ash eruption of 18 May, even if a first phreatic eruption took place on March 28 (Endo *et al.*, 1981). At Mt. Redoubt volcano, the maximum observed magnitude was about 2.0, and seismic activity began just a few hours before the eruption (Benoit and McNutt, 1996). During the eruptive crisis at Mt. Pinatubo in 1991, about a dozen earthquakes with magnitudes >3.0 were observed, but in that case the monitoring network was installed when the seismic activity was already intense and in progress (Murray *et al.*, 1997).

Because the above catalogs are reliable for a magnitude $M > 3$, we can define how many events with magnitudes in this range, that is, $N(M > 3)$, should be represented in our catalog. The dimension of the latter (N_{M_0} , i.e., $N[M > 2.0]$) can be obtained by scaling the chosen value as a function of b . We set $N(M > 3) = 80$, corresponding to $N_{M_0} = 8000$, for $b = 2.0$.

The maximum magnitude in this catalog is 4.3, comparable to the values recorded during the preeruptive phases of some significant eruptions (Table 1). Because variations of N_{M_0} and b are expected to affect our results significantly, we allowed these parameters to vary to also establish some levels of uncertainty in the final values. Specifically, we generated four additional catalogs, using $b = 1.5$ and $b = 2.5$ for fixed $N_{M_0} = 8000$ and $N_{M_0} = 1000$ (10 events with $M > 3$), and $N_{M_0} = 40,000$ (400 events with $M > 3$) for fixed $b = 2.0$. We noted that a change of one order of magnitude in the N_{M_0} value approximately corresponds to a variation of one unit in the a value of the G–R relationship.

Synthetic Seismograms

For any event in the catalog (i.e., for each magnitude), a synthetic seismogram has been computed. The adopted simulation technique was the discrete wave-number method

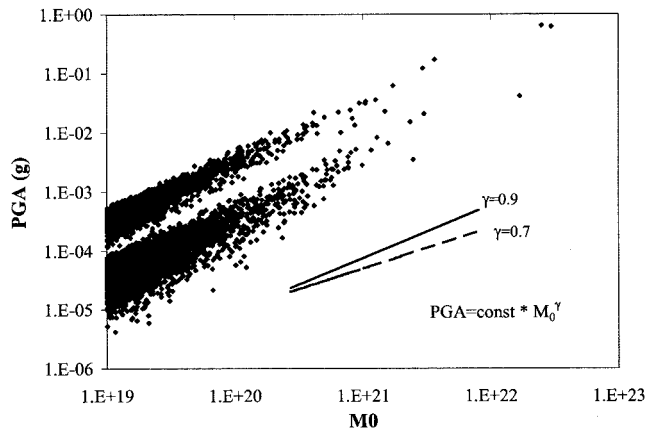


Figure 1. Simulated PGA values and comparisons with attenuation laws available from the literature (De Natale *et al.*, 1988).

Table 1
Maximum Magnitudes Observed during Preeruptive Phases of Some of the World's Volcanoes*

Volcano (year of eruption)	M_{MAX}
Mt. St. Helens (1980)	5.1
Pinatubo (1991)	4.3
Kilauea (1998)	4.2
Mt. Spurr (1992)	1.7
Redoubt (1989)	2.0

*From Benoit and McNutt (1996).

(Bouchon, 1980), numerically implemented by Coutant (1989). This method computes Green's functions in the frequency domain for a flat-layered half-space, using potentials in cylindrical coordinates and convolving them for the source time history. The final accelerograms were computed for a site 8 km away from the cone axis—that is, corresponding to the town of Portici, which is the most densely inhabited town in the Vesuvius area. Although this method has the disadvantage of considering very simple, flat-layered media, without specific topography, it has the major quality of computing the complete seismic wave field with a relatively low computation time, also for signals having frequencies higher than 1 Hz. In contrast, the massive use of full wave-field, three-dimensional methods would require significant computation time with an allowed maximum frequency lower than 1 Hz for realistic media (Pitarka, 1999).

The velocity model used for the Mt. Vesuvius volcano and the surrounding areas was a simplified representation of the tomographic models recently obtained by De Matteis *et al.* (2000) and Zollo *et al.* (2002). The background model is a three-layer medium, with a superficial low-velocity layer with $V_p = 1.7$ km/sec, an intermediate one with $V_p = 3.3$ km/sec, and the half-space with $V_p = 6.0$ km/sec. This velocity model approximates the geological structure of the volcanic area, with a shallow volcanic/alluvial sedimentary formation overlying the Mesozoic carbonate basement. To simulate the real seismogram complexity, the superficial layer was split into a large number of thin layers, with random velocity inversions. This trick allows the reduction of the amplitude of the resonance waves trapped in the superficial layer, which are produced by the 1D layering of the medium without significantly modifying the values of the strong-motion parameters.

A double-couple, point-source earthquake model was assumed, owing to the relatively small rupture surface of events in the considered magnitude range (hundreds of meters) with respect to the distances between source and receiver. Moreover, a single pulse with a triangular-source time function was used, the amplitude of which is related to the seismic moment of the earthquake. The source-function duration was calculated by assuming a circular rupture area (Sato and Hirasawa, 1973), with a stress-drop value of 4 MPa (Zollo *et al.*, 2002). Random fault orientations and slip directions (strike, dip, and rake) (Aki and Richards, 1980) are assumed, since no preferential rupture and/or mechanism orientation of earthquakes would be expected during the pre-rupture phase. The earthquake sources have been located along the vertical axis of the volcanic vent, at depths between 0 and 4.0 km. These locations are consistent with the spatial distribution of the real earthquakes at Mt. Vesuvius over the last decades (Zollo *et al.*, 2002).

Validation of Synthetic Waveform Modeling

Synthetic seismograms computed with the discrete wave-number method are a simplified representation of the

complete wave field because they do not account for the topography, site effects, and possible fault surfaces of finite length. However, the expected rupture sizes are much smaller than the considered source-receiver distances (8–10 km from the hypocenter), and the smooth topography of Mt. Vesuvius was expected to produce mainly low-frequency diffraction effects.

To verify the quality of our results, we have compared synthetic seismograms with real data recorded in the Vesuvius area. The available seismic database is a collection of earthquakes with magnitudes larger than 3.0, recorded by the Vesuvian Observatory Net since 1972, using three-component Lennharz 2-Hz seismographs, and stations along the volcano slopes 1–2 km away from the crater. The comparison was made to verify whether synthetic seismograms were able to reproduce strong-motion parameters that are relevant for structural-damage evaluation. Apart from the classical indicators, such as peak ground acceleration (PGA) and peak ground displacement (PGD), other parameters were also compared: response spectra, Arias intensity (Arias, 1970), and effective duration as defined by Trifunac and Novikova (1995). For a complete description of these parameters and their application to engineering purposes, we refer to Cosenza and Manfredi (2000).

The first control of the reliability of the numerical simulations was performed in terms of the PGA scaling with the seismic moment. In Figure 1 the synthetics are plotted with attenuation laws available from the literature (Boore, 1983; De Natale *et al.*, 1988). Specifically, the scaling law inferred by De Natale *et al.* (1988) concerns the earthquake sequence that occurred in the Phlegrean Fields volcanic area during the unrest crisis of 1982–1984.

In Figures 2, 3, and 4, the PGD, the intensity of Arias (I_A), and the duration of Trifunac and Novikova (d_{TN}) are plotted as functions of the magnitude for both synthetic and observed records (in this comparison, the synthetic dataset has been limited to the events having magnitudes larger than 3.0). For PGD and I_A , the amplitudes of real and synthetic seismograms have been scaled with respect to the epicentral distance to cancel the effects of geometrical spreading.

In Figures 1 and 3, two distinct trends for the attenuation laws can be seen. If the source is in the intermediate layer (representing the low-velocity thick formation of volcanic and alluvial sediments of the Campanian Plain), PGA and Arias intensity are one order of magnitude larger than the corresponding values obtained when the source is in the bottom layer (high-velocity Mesozoic limestone basement). Moreover, for shallow sources, the maximal ground motion in terms of both acceleration and displacement occurs within a secondary *S*-wave train; the waves are indeed trapped in the shallow layers, and resonance and multiple-reflection effects are dominant. Otherwise, when the source is deeper, the maximum amplitudes occur in the direct *S* waves.

Considering d_{TN} and PGD, a scattering in both data and synthetics can be observed (Figs. 2, 4). Generally, synthetics underestimate the duration when compared with data. The

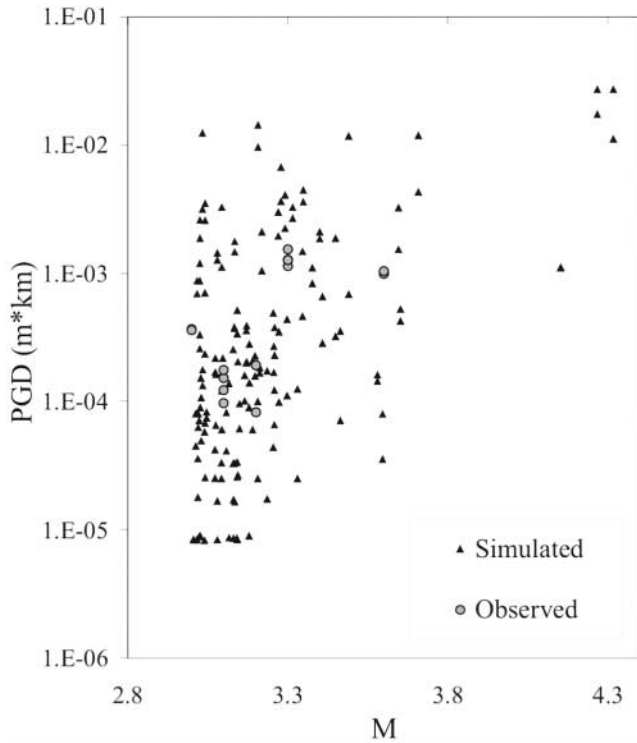


Figure 2. PGD values for both synthetics and data as a function of magnitude. Seismograms are appropriately scaled for the epicentral distance to remove the effects of geometrical spreading.

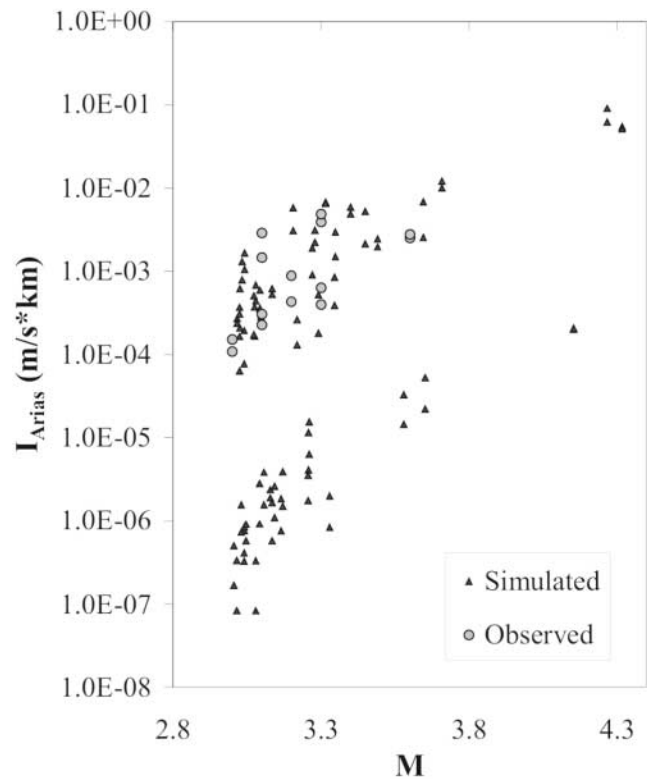


Figure 3. Arias (1970) intensity I_A values for both synthetics and data as a function of magnitude. Seismograms are appropriately scaled for the epicentral distance to remove the effects of geometrical spreading.

wave field in the observed signals is likely to be scattered as an effect of the subsoil heterogeneities and/or topographic diffractions; thus it is very difficult to reproduce the duration, starting from a simple, flat-layered velocity model. In Figure 5, a comparison of the scaled acceleration response spectra is shown for the observed and simulated seismograms, along with the envelope of all of the simulated records for magnitudes varying from 3 to 3.4. We show that the spectral shapes of simulated events satisfactorily match the real ones; the spectral amplification in the low-period range ($T < 0.2$ sec), especially, is well reproduced by the synthetic seismograms. Again, the synthetic envelopes for deeper events underestimate the real ones.

Possible Damage to Structures

The simulation of the preeruptive phase, using the mean values of parameters $b = 2.0$ and $N_m = 8000$, originated in about 80 events of magnitude $M > 3$. The corresponding maximum values of the ground-motion parameters are relatively small, and no relevant damage would be expected for a single event in the preeruptive phase (even if the maximum event in the catalog ($M = 4.3$ in Table 2) is considered).

The analysis of acceleration-response spectral shape (Fig. 5) clearly indicates that the amplification is significant in the low-period range ($T < 0.2$ sec). This means that struc-

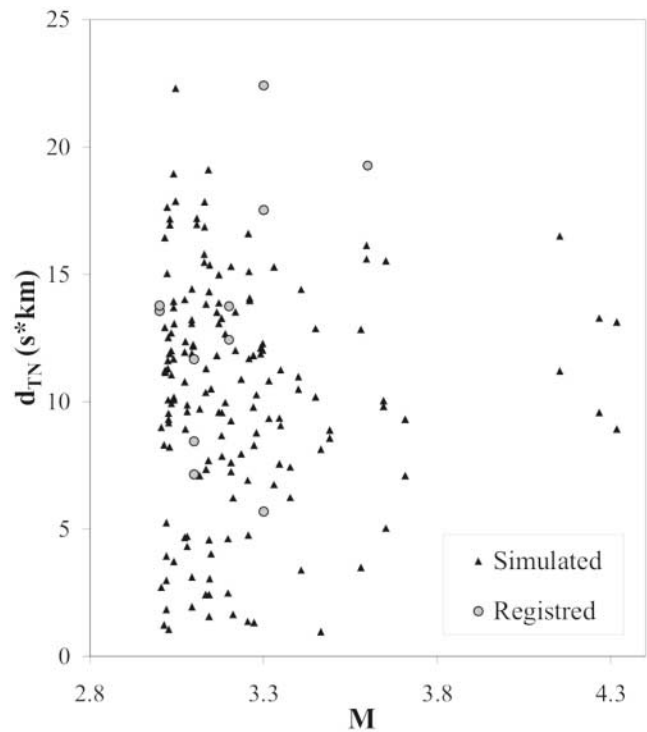


Figure 4. Comparisons of observed and simulated d_{TN} values as a function of magnitude.

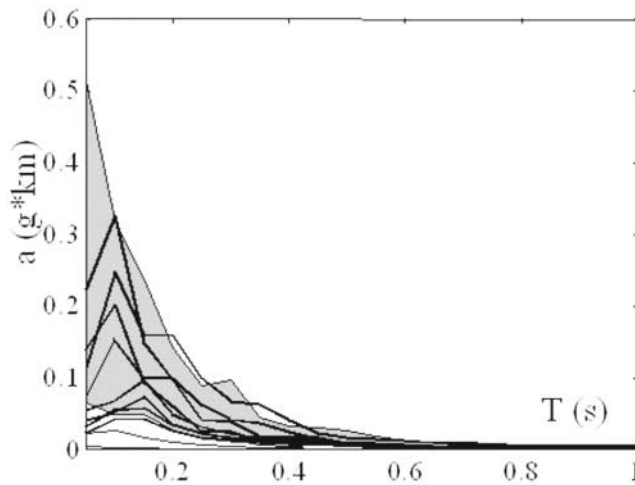


Figure 5. Comparisons of response spectra for simulated (shaded envelopes) and observed events, scaled as a function of epicentral distance. The dark-gray zone is related to events in the shallow zone, and the light-gray zone is associated with deeper events. All the events belong to the catalog generated for $b = 2.0$, $N_{M_0} = 40,000$.

Table 2
Maximum Values of Parameters in the Synthetic Seismic Sequence

b	N_{M_0}	M	PGA (g)	PGV* (m/s)	PGD (cm)	I_A (m/s)
2.5	8,000	4.0	0.061	0.009	0.3	0.006
2.0	1,000	3.69	0.032	0.004	0.2	0.0015
2.0	8,000	4.3	0.066	0.018	0.2	0.011
2.0	40,000	4.5	0.101	0.028	0.3	0.026
1.5	8,000	5.1	0.293	0.091	0.8	0.212

The different catalogs are classified as functions of the parameters b (the Gutenberg–Richter slope) and N_{M_0} (their dimension).

*Peak ground velocity.

tures with a very low fundamental period are the candidates for damage owing to cumulative effects. These structures correspond to very stiff or low-rise structures, such as masonry buildings and reinforced-concrete structures with one or two floors.

Cumulative Effects

Although a single seismic event of a preeruptive phase may not be relevant in terms of damage to buildings, the cumulative effect of a large number of events taking place over a few days before an eruption can cause structural damage. In fact, damage is not only caused by peak strength or displacement demand but is often related to the exhaustion of energy-dissipation capacity caused by an excessive number of plastic-cycle reversals imposed to the structure (low-cycle fatigue).

On the other hand, the effects of a very large number of elastic cycles (high-cycle fatigue) also influence the seismic response. This response acts on nonstructural parts (e.g., infill panels in strategic buildings, bearing devices in bridges) of critical facilities and of lifelines. The functionality of the infrastructure is indeed crucial for the planning of emergency activities in the preeruptive phase.

Low-cycle fatigue is a significant cause of damage of badly designed structures, such as traditional masonry and low-rise reinforced-concrete buildings. In these cases, the cyclic collapse of the structures can be described by the demand of the hysteretic energy E_h (Manfredi, 2001; Manfredi *et al.*, 2003). This represents the amount of input energy that should be dissipated by the plastic behavior of the structures (with inelastic deformations), and it is not recoverable. According to the energy criterion, the structure collapses when the hysteretic energy demand exceeds the allowable plastic energy $E_{h,alw}$ for the structure (Uang and Bertero, 1990). Different studies are available for the assessment of allowable hysteretic energies in structural elements (Darwin *et al.*, 1986).

The spectrum of hysteretic energy (hysteretic energy vs. building-vibration period) can be derived for a given level of system yielding strength F_y that represents the threshold level during the transition of the structure from the elastic to the plastic state. We have chosen $F_y = 0.05 g$, which is representative of the seismic capacity of a large class of badly designed structures affected by ground-motion amplification in the high-frequency range.

In Figure 6, the hysteretic-energy spectrum for the main events predicted for the scenario ($b = 2.0$, $N_m = 40,000$) is shown (by definition, the hysteretic energy is an additive quantity). The effect of energy accumulation is significant, as the global E_h is approximately 3 times larger than that corresponding to the single largest event. As they are directly connected to the maximum elastic demand of the system, the hysteretic energy spectra decrease with period T ; thus, the stiffer structures ($T \leq 0.2$ sec), again, should suffer major damage from these cumulative effects.

If we choose a higher yielding limit for the system, the plastic-energy demand decreases; for instance, $F_y = 0.1 g$ corresponds to a peak energy demand of 0.016 joule/kg, which is twice as large as that associated with the single largest event. This means that the contribution of weak events becomes less important for stronger structures.

In Figure 7, the variation in the global hysteretic energy spectra for the simulated scenarios is compared with the observed E_h spectra at $F_y = 0.05 g$ at station Assisi Scalone (west-east component) during the 1997 Umbria Marche earthquake ($M 5.6$, $PGA = 0.16 g$, $I_A = 0.11$ m/sec). Because hysteretic-energy demand is comparable to the Marche–Umbria earthquake, the expected damage to the buildings in the area surrounding Mt. Vesuvius should be relevant when considering the damage observed in the area affected by this previous earthquake.

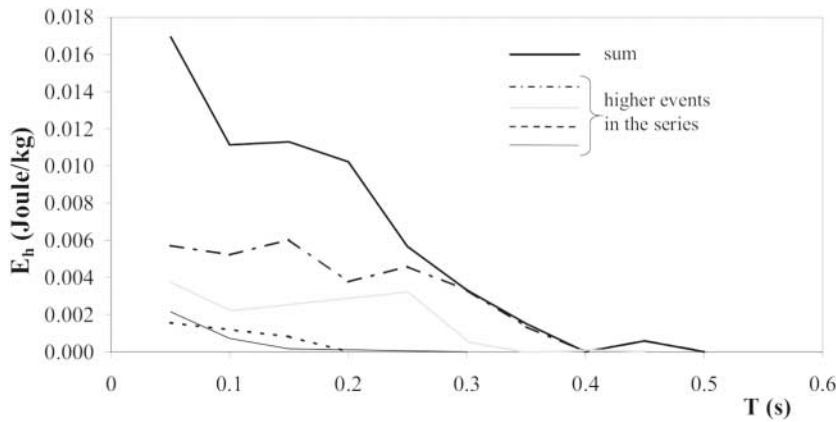


Figure 6. Hysteretic-energy spectrum for $b = 2.0$, $N_{M_0} = 40,000$ scenario. The cumulative effects of the whole preeruptive series (solid black line) is compared with the single most energetic events in the series. The spectrum equates to the strength characteristics of badly designed brittle structures ($F_y = 0.05 g$).

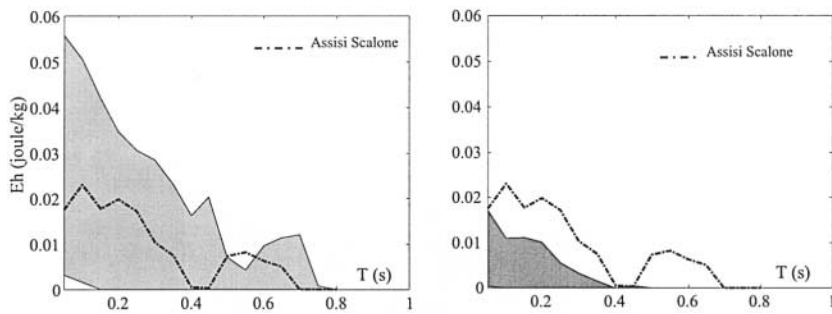


Figure 7. Hysteretic-energy spectra and comparisons with the Assisi Scalone WE component of the 1997 Umbria–Marche earthquake. In the left panel, lower and upper boundaries of the shadow zone correspond to the catalogs obtained from $b = 2.5$ and $b = 1.5$, respectively, with $N_{M_0} = 8000$. In the right panel, lower and upper boundaries are associated with catalogs ($b = 2.0$, $N_{M_0} = 1000$) and ($b = 2.0$, $N_{M_0} = 40,000$). The b -parameter has a larger influence on the variation of E_h than N_{M_0} .

We note that a possible variation in parameter b can significantly affect the peak energy demand, with values comparable to or higher than those observed during a moderate-sized earthquake in the Apennines; the variation in the parameter N_m is less important.

Conclusions

The evaluation of seismic hazards related to preeruptive seismic sequences is an innovative approach in the study of seismic and volcanic hazards in active volcanic areas near dense urban centers. In this context, this study is a first trial aimed at linking the two aspects of earthquake simulation and structural-engineering interpretation for the case of volcanic earthquakes that would potentially occur before an eruption of Mt. Vesuvius.

To rely on an earthquake catalog representing the preeruptive phase, it was necessary to build a synthetic database and to validate it through comparisons with observed records. The ground-motion simulations produced reliable results in terms of peak demand (PGA, PGD), spectral shape, and integral parameters (Arias intensity). On the other hand, the effective duration of the synthetic waveforms is systematically underestimated owing the use of a simplified 1D velocity model.

This study demonstrates the relevance of the source location relative to the velocity-structure discontinuities, because the shallower events would be expected to produce

waveforms with ground-motion durations and peak values significantly different from deeper events. This emphasizes the importance of obtaining accurate event–depth estimates and warns against using the whole dataset for estimating the attenuation-law parameters in areas where seismic discontinuities with strong impedance contrasts are well recognized (in this case, volcanic sediments on a limestone basement).

With regard to possible structural effects, both the larger magnitude events and the cumulative effects of the whole preeruptive series are considered. It is of note that possible variations in the Gutenberg–Richter law parameters (b and N_m) can have significant influences, both in terms of peak events and of global energy content of the entire series.

The simulated response spectra for single events show amplifications in the low-period range ($T < 0.2$ sec). Therefore, very stiff structures (such as masonry buildings or low-rise reinforced-concrete-frame structures) are expected to be affected during the preeruptive earthquake occurrence.

The cumulative hysteretic-energy demand is representative of the plastic behavior of the structures, and it can provide a first-order estimation of damage effects. The comparison between the cumulative hysteretic energy as inferred from our simulation and the observed spectrum during a moderate-sized earthquake in the Apennines (1997, Umbria–Marche earthquake, $M 5.6$) shows that they can attain comparable levels. We note that extended building damage was observed as a consequence of the Umbria–Marche earthquake, whereas relatively small values of peak ground-

motion parameters were recorded. Moreover, considering the range of global E_h variation for the different scenarios considered, the importance of the b -value is confirmed, its having also determined significant differences in terms of peak energy demand.

Based on these grounds, it can be concluded that an entire series of preeruptive earthquakes can cause structural damage because of the low-cycle-fatigue phenomenon. Similar effects of damage to civil structures were observed during the last 1982–1984 ground-uplift episode in the town of Pozzuoli (inside the caldera of Campi Flegrei), 15 km west of Naples. The ground-deformation episode was accompanied by an intense, shallow seismic activity, consisting of more than 20,000 micro-earthquakes with magnitudes between -1 and 4 , located at depths shallower than 3–5 km (Aster and Meyer, 1988). The damage to buildings produced by the inflating-soil phenomenon and by the intense, shallow seismic activity, and also the fear of a possible opening of an eruptive vent, led the authorities to evacuate large parts of the town of Pozzuoli, where the maximum ground uplift was observed.

According to this recent experience, strategic facilities and transportation infrastructure can be put out of service, thus preventing their use, which is crucial for emergency management. A careful investigation of infrastructure behavior should be carried out, along with the need for re-establishing minimal design requirements to have acceptable functionality from a performance-based design point of view. Furthermore, new research is needed to evaluate the effects of a large number of elastic cycles (high-cycle fatigue) on the serviceability of the structures.

Acknowledgments

We thank P. Gasparini for helpful comments and suggestions. This work has been financially supported by MIUR-FISR and by the Department of Civil Protection through the Gruppo Nazionale Difesa dei Terremoti (INGV).

References

- Aki, K., and P. G. Richards (1980). *Quantitative Seismology*, W. H. Freeman, San Francisco.
- Arias, A. (1970). A measure of earthquake intensity, in *Seismic Design of Nuclear Power Plants*, MIT Press, Cambridge, Mass., 438–468.
- Aster, R., and R. Meyer (1988). Three-dimensional velocity structure and hypocenter distribution in the Campi Flegrei caldera, Italy, *Tectonophysics* **149**, 195–218.
- Benoit, P., and S. R. McNutt (1994). A volcanic earthquake database, European Seismological Commission Workshop on Seismic Signals on Active Volcanoes, Possible Precursors of Volcanic Eruptions, Nicotoli, Italy.
- Benoit, P., and S. R. McNutt (1996). Global volcanic earthquake swarm database 1979–1989, *U.S. Geol. Surv. Open-File Rept.* 96-69.
- Boore, D. M. (1983). Stochastic simulation of high frequency ground motions based on seismological models of the radiated spectra, *Bull. Seism. Soc. Am.* **73**, 1865–1894.
- Bouchon, M. (1980). A simple method to calculate Green's functions for elastic layered media, *Bull. Seism. Soc. Am.* **71**, 959–971.
- Bury, K. V. (1975). *Statistical Models in Applied Science*, Wiley, New York.
- Chouet, B. A., R. A. Page, C. D. Stephens, J. C. Lahr, and J. A. Power (1994). Precursory swarms of long-period events at Redoubt volcano (1989–1990), Alaska: their origin and use as forecasting tool, *J. Volc. Geoth. Res.* **62**, 95–135.
- Cosenza, E., and G. Manfredi (2000). Damage indices and damage measures, in *Progress in Structural Engineering and Materials*, Vol. 2, Wiley, New York.
- Coutant, O. (1989). Program of Numerical Simulation AXITRA, Res. Report LGIT, Grenoble (in French).
- Darwin, D., and C. K. Nmai (1986). Energy dissipation in RC beams under cyclic load, *J. Struct. Eng.*, ASCE, **112**, 1829–1846.
- De Matteis, R., D. Latorre, A. Zollo, and J. Virieux (2000). 1-D P -velocity models of Vesuvius volcano from the inversion of TomoVes96 first arrival time data, *Pageoph.* **157**, 1643–1661.
- De Natale, G., S. Gresta, G. Patané, and A. Zollo (1985). Statistical analysis of earthquake activity at Etna volcano (March 1981 eruption), *Pageoph.* **123**, 697–705.
- De Natale, G., E. Faccioli, and A. Zollo (1988). Scaling of peak ground motions from digital recordings of small earthquakes at Campi Flegrei, southern Italy, *Pageoph.* **126**, 37–53.
- Endo, E. T., S. D. Malone, L. L. Noson, and C. S. Weaver (1981). Locations, magnitudes, and statistics of the March 20–May 18 earthquake sequence, in *The 1980 Eruption of Mount St. Helens, Washington*, P. W. Lipman and D. R. Mullineaux (Editors), *U.S. Geol. Surv. Prof. Pap.* 1250, 93–107.
- Manfredi, G. (2001). Evaluation of seismic energy demand, *Earthquake Eng. Struct. Dyn.* **30**, 485–500.
- Manfredi, G., M. Polese, and E. Cosenza (2003). Cumulative demand of the earthquake ground motions in the near source, *Earthquake Eng. Struct. Dyn.* **32**, 1853–1865.
- Minakami, T. (1974). Seismology of volcanoes in Japan, in *Physical Volcanology Developments in Solid Earth Geophysics*, Vol. 6, L. Civetta (Editor), Elsevier, Amsterdam, 1–27.
- Murray, T. L., J. A. Power, G. D. March, and J. N. Marso (1997). A PC-based real-time volcano-monitoring data-acquisition and analysis system, in *Fire and Mud, Eruption and Lahars of Mount Pinatubo, Philippines*, C. G. Newhall and R. S. Punongbuyan (Editors), Univ. of Washington Press, Seattle.
- Pitarka, A. (1999). 3D elastic finite-difference modeling of seismic motion using staggered grids with nonuniform spacing, *Bull. Seism. Soc. Am.* **89**, 54–68.
- Power, A. J., M. Wyss, and J. L. Latchman (1998). Spatial variations in the frequency-magnitude distribution of earthquakes at Soufriere Hills volcano, Monserrat, *Geophys. Res. Lett.* **25**, 3653–3656.
- Reiter, L. (1991). *Earthquake Hazard Analysis: Issues and Insights*, Columbia Univ. Press, New York.
- Sabetta, F., and A. Pugliese (1987). Attenuation of peak horizontal acceleration and velocity from Italian strong-motion records, *Bull. Seism. Soc. Am.* **77**, 1–23.
- Sato, T., and T. Hirasawa (1973). Body wave spectra from propagating shear cracks, *J. Phys. Earth* **21**, 415–431.
- Trifunac, M. D., and E. I. Novikova (1995). State of the art review on strong motion duration, in *Proc. of the 10th European Conf. on Earthquake Engineering*, Rotterdam.
- Uang, C. M., and V. V. Bertero (1990). Evaluation of seismic energy in structures, *Earthquake Eng. Struct. Dyn.* **19**, 77–90.
- Wiemer, S., and S. R. McNutt (1997). Variations in the frequency-magnitude distribution with depth in two volcanic areas: Mount St. Helens, Washington, and Mount Spurr, Alaska, *Geophys. Res. Lett.* **24**, 189–192.
- Zollo, A., W. Marzocchi, P. Capuano, A. Herrero, A. Lomax, and G. Iannaccone (2002). Space and time behavior of seismic activity at Mt. Vesuvius volcano, southern Italy, *Bull. Seism. Soc. Am.* **92**, 625–640.

U-RISSC, Unità de Ricerca in Sismologia Sperimentale e Computazionale
Dipartimento di Scienze Fisiche
Università "Federico II"
via Coroglio, 256
80124 Napoli
(G.F., A.Z.)

Departement de Sismologie
Institut de Physique du Globe du Paris
4, Place Jussieu
75252 Paris cedex 05
(G.F.)

Dipartimento Analisi e Progettazione Strutturale
Università "Federico II"
via Claudio 21
80125 Napoli
(G.M., M.P., E.C.)

Manuscript received 21 April 2003.